EARTH-BASED S-BAND RADAR MAPPING OF THE MOON: NEW VIEWS OF IMPACT MELT DISTRIBUTION AND MARE PHYSICAL PROPERTIES. B.A. Campbell[1], L.M. Carter[1], D.B. Campbell[2], M. Nolan[3], J. Chandler[4], R.R. Ghent[5], B.R. Hawke[6], R.F. Anderson[1], and K. Wells[2], [1]Smithsonian Institution, Center for Earth & Planetary Studies, Washington DC 20013-7012, campbellb@si.edu, [2]Cornell University, Ithaca, NY 14853, [3]Arecibo Observatory, Arecibo, PR 00612, [4]Smithsonian Astrophysical Observatory, Cambridge, MA 02138, [5]University of Toronto, Toronto, ON, [6]HIGP, University of Hawaii, Honolulu, HI 96822.

Introduction: We present results at the halfway point of a campaign to map much of the Moon's near side using the 12.6-cm radar transmitter at Arecibo Observatory and receivers at the Green Bank Telescope. These data have a single-look spatial resolution of about 40 m, with final maps averaged to an 80-m, four-look product to reduce image speckle (Fig 1).

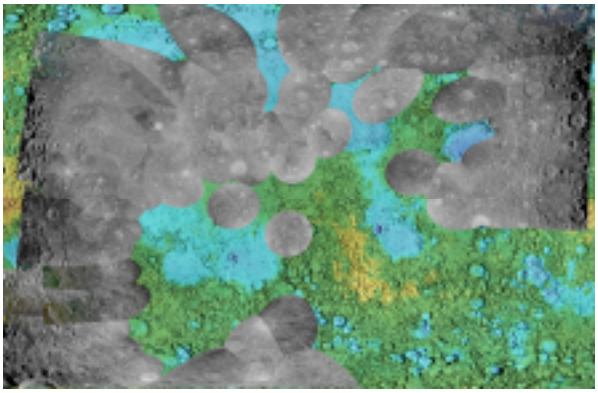

Fig. 1. Coverage through 2009 of the lunar nearside by S-band radar mapping; greyscale radar images on color shaded-relief background.

Focused processing is used to obtain this high spatial resolution over the entire region illuminated by the Arecibo beam. The transmitted signal is circularly polarized, and we receive reflections in both senses of circular polarization; measurements of receiver thermal noise during periods with no lunar echoes allow well-calibrated estimates of the circular polarization ratio (CPR) and the four-element Stokes vector. Radiometric calibration to values of the backscatter coefficient is ongoing. Radar backscatter data for the Moon provide information on regolith dielectric and physical properties, with particular sensitivity to ilmenite content and surface or buried rocks with diameter of about one-tenth the radar wavelength and larger.

Mare Physical Properties: Fig. 2 shows the mean behavior of the CPR for mare units at 30°-50° incidence angle over a wide range of titanium content. The solid line denotes the best-fit functional dependence of 70-cm echoes for the same geometry [1]. The large offset with wavelength is not unexpected; Hagfors [2] shows that the disk-integrated CPR for 68-cm wavelength reaches a maximum of about 0.4-0.5 toward the limb (grazing incidence), while 23-cm echoes reach a maximum CPR of 0.5-0.6, with the asymptotic behavior occurring at smaller incidence angles for shorter wavelength.

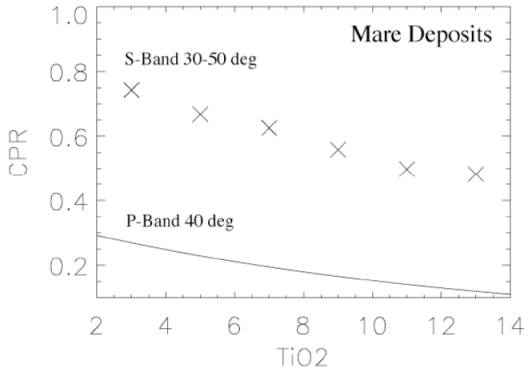

Fig. 2. Circular polarization ratio values at 12.6-cm wavelength (crosses) based on averages over mare regions of Fig. 1. Solid line is approximate behavior of the nearside maria at 70-cm wavelength [1].

The circular polarization ratios measured for the lunar maria at low TiO_2 content are higher than those of rough terrestrial lava surfaces, which have an asymptotic limit in CPR value of about 0.6 for 60° incidence angle [3]. CPR values of 0.5 to >1 are frequently observed in 12.6-cm and 70-cm radar echoes of proximal lunar crater ejecta, and for some apparently rugged volcanic deposits [4], but the mare surfaces are not particularly rough at the decimeter scale. The enhanced CPR values across the maria are likely due to a substantial contribution of diffuse scattering from rocks suspended in the fine-grained regolith matrix - a mechanism long suggested to explain the generally higher backscatter cross sections than predicted by surface rocks alone [5].

Impact Melt from Craters: An outflow deposit, inferred to be impact melt, from Glushko crater (Fig. 3) has CPR values near unity at 12.6-cm and 70-cm wavelengths (Fig. 4) and thus a very rugged near-surface structure at the decimeter to meter scale. This deposit does not show radar-brightness variations consistent with levees or channels, and appears to nearly overtop a massif, suggesting very rapid emplacement. Deposits of similar morphology and/or radar brightness are noted for craters such as Pythagoras, Rutherfurd, Theophilus, and Aristillus.

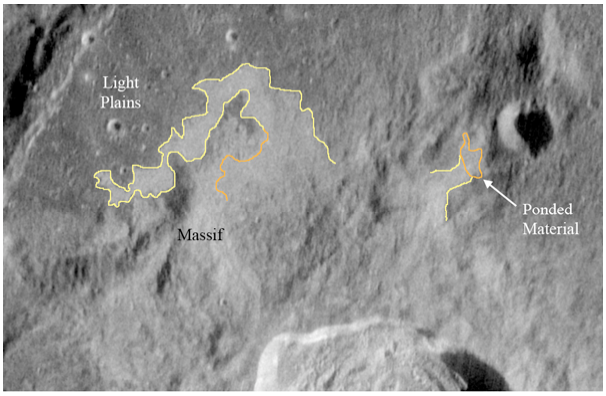

Fig. 3. S-band same-sense circular polarization (SC) radar image of Glushko crater (43 km diameter) northern rim and ejecta deposits. Yellow outlines indicate bounds of rough, radar-bright flows delineated from radar image; orange outlines show limits inferred from smooth regions in photographic data. Note partial overtopping of the north-trending massif at left center by radar-bright material.

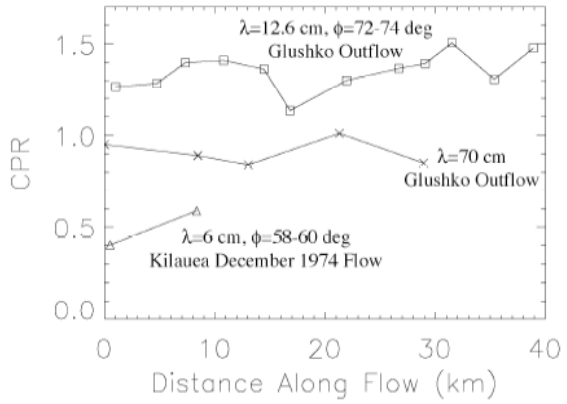

Fig. 4. Circular polarization ratio, at 12.6-cm and 70-cm wavelengths, versus distance from the outer margin of the continuous ejecta for the Glushko crater outflow deposit. For comparison, CPR values at 6-cm wavelength for the pahoehoe/aa transition in the December 1974 Kilauea lava flow are also plotted.

Orientale Impact Melt Distribution: Impact melt deposits appear to extend to great distances for basin-scale events, as shown by 70-cm mapping of radar-bright, high-CPR small crater clusters in smooth areas mapped as Imbrian-period plains units across the south polar region [6, 7]. The enhanced radar backscatter from these small craters, attributed to a dense regolith substrate provided by cooled impact melt from Orientale, were revealed in greater detail by 12.6-cm images of the south pole [8]. Favorable libration for viewing the lunar north pole from Arecibo, which had been very limited in the past several years, occurred again in 2009, so we now have a comparison image showing the polarization properties of this area.

Images of the north pole show that, despite recording the deposition of Orientale material, Byrd and Peary craters do not have dense patterns of radar-bright ejecta from small craters on their floors (Fig. 5). Such patterns in Amundsen crater, near the south pole, were interpreted as diagnostic of abundant impact melt, so the fraction of Orientale-derived melt in the north polar smooth plains, 1000 km farther from the basin center, is inferred to be much lower.

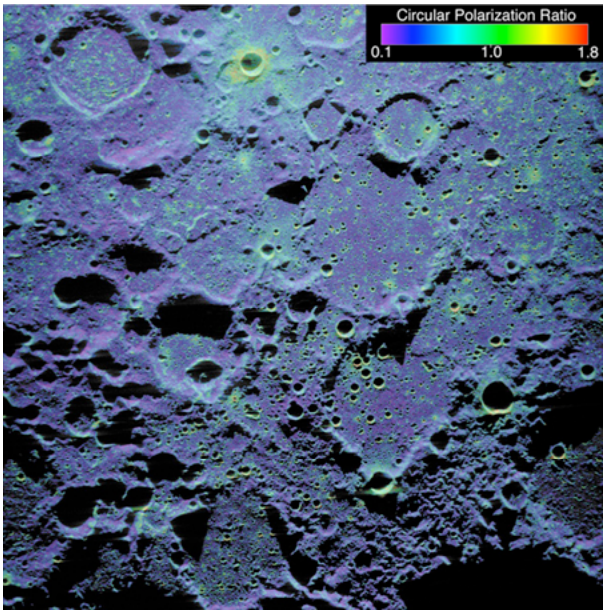

Fig. 5. S-band opposite-sense circular (OC) radar backscatter image of the north polar region of the Moon, with circular polarization ratio as color overlay. Polar stereographic projection; image width 365 km. Zero longitude toward top center.

References: [1] Campbell, B.A., et al. (2009) GRL, 36, L22201, doi:10.1029/2009GL041087; [2] Hagfors, T. (1970) Radio Science 5, 189-227; [3] Campbell, B.A. (2009) IEEE Trans. Geosci. Rem. Sensing 47, 3480-3488, doi:10.1109 / TGRS.2009.2022752; [4] Campbell, B.A., Hawke, B.R., and Campbell, D.B.. (2009) JGR, E01001, doi:10.1029/2008JE003253; [5] Thompson, T.W. (1974) The Moon 10, 51-85; [6] Campbell, B.A., and Campbell, D.B., (2006) Icarus 180, 1-7; [7] Ghent, R.R., et al., (2008) Geology 36, 343-346, doi:10.1130/G24325A.1; [8] Campbell, D.B., et al., (2006) Nature 443, 835-837.